Biomaterials Science

COMMUNICATION

View Article Online
View Journal | View Issue





Cite this: *Biomater. Sci.*, 2018, **6**, 997

Received 30th November 2017,
Accepted 11th February 2018

DOI: 10.1039/c7bm01114h

rsc.li/biomaterials-science

# Light-triggered release of drug conjugates for an efficient combination of chemotherapy and photodynamic therapy†

Lin Liu,‡[a] Ruibo Wang,‡[b] Chunran Wang,[a] Jinze Wang,[a] Li Chen *[a] and Jianjun Cheng [b]

**Herein, we present a series of light-triggered porphyrin-based polymeric drug conjugates PSDTD-*m* for combined chemo-photodynamic therapy of cancer. The controlled release of a drug through a ROS-cleavable linker combined with photodynamic therapy showed enhanced anticancer efficacy, proving the effectiveness of this light triggered smart nanocarrier platform for enhancing the therapy efficacy.**

In current cancer therapy strategies, chemotherapy is still the major therapeutic modality. However, many chemotherapy drug molecules have limited clinical use due to their poor water solubility, short circulation half-life and severe cytotoxicity to healthy organs.[1–4] To address these problems, a variety of nanomaterials, including lipids, polymers, and silica oxides, have been actively exploited as drug delivery carriers.[5–9] Drugs can either be physically encapsulated or chemically conjugated to these carriers. These nano-sized drug delivery systems bring benefit to chemotherapy drugs including improved solubility, enhanced plasma circulation half-life, alleviated toxicity and upregulated antitumor efficacy. To realize on-demand drug release only at the targeted site, stimuli-responsive nanocarriers have been developed for "triggered" drug release in response to extracorporeal physical stimuli (temperature,[9] light,[10] and ultrasound[11,12]) or intracorporeal chemical stimuli (acid,[13] enzyme,[14] and redox[15]). Among these stimulations, light has been considered an attractive way to trigger the drug release at the pathological location due to its precise controllability.[16]

To obtain a better therapeutic efficacy, chemotherapy also has been synergistically combined with other treatment methods such as photodynamic therapy (PDT), gene therapy, photothermal therapy and so on.[17–19] The combination of two therapeutic modalities brings a synergistic effect to overcome the limitations of a single therapy. It is reported that the combination of PDT with chemotherapy can shorten the overall treatment time, reduce side effects and induce antitumor immunity.[20] PDT is a highly controllable treatment for many cancers. Under light irradiation of a specific wavelength, a photosensitizer can generate singlet oxygen or reactive oxygen species (ROS) to kill cancer cells.[21–25] In particular, porphyrins and their derivatives have been well-studied as a class of promising materials to generate ROS and kill tumor cells. Our group had developed smart nanoparticles based on metallo-supramolecular interactions between metalloporphyrins and histidine grafted on dextran and realized co-encapsulation of drug and photosensitizer with acid-sensitive drug release.[26–28] In these reported studies, the photosensitizer, metalloporphyrins, was loaded into nanoparticles by non-covalent interactions and the drug was physically encapsulated. However, the premature drug release in blood circulation and unwanted side effects hindered further development of these nanoparticle platforms for efficient combination therapy. In this work, we developed dextran-based polymeric drug conjugates PSDTD-*m* to tackle these problems and achieve an efficient combination of chemotherapy and PDT.

As shown in Scheme 1, dextran, a polysaccharide consisting of 1,6-, and 1,3-glucosidic linkages, was used as the hydrophilic backbone. It is widely used as a drug delivery material due to its definite biocompatibility, biodegradability and hydrophilicity. In addition, dextran possesses multiple hydroxyls which are convenient for chemical modification to endow nanoparticle surfaces with various desired functions. Porphyrin and drug were chemically conjugated on the dextran backbone to address premature drug release. The anticancer drug doxorubicin (DOX) was conjugated with dextran through a ROS cleavable thioketal (TK) linker while porphyrin molecules were conjugated with an ester linker. These drug conjugates can self-assemble to form micellar nanoparticles. In these smart nanoparticles, porphyrin molecules would generate cytotoxic ROS under light irradiation. Simultaneously, the

[a]*Department of Chemistry, Northeast Normal University, Changchun 130024, P. R. China. E-mail: chenl686@nenu.edu.cn; Fax: +86 431 85099668; Tel: +86 431 85099667*

[b]*Department of Materials Science and Engineering, University of Illinois at Urbana-Champaign, Urbana, Illinois 61801, USA*

†Electronic supplementary information (ESI) available. See DOI: 10.1039/c7bm01114h

‡These authors contributed equally to this work.

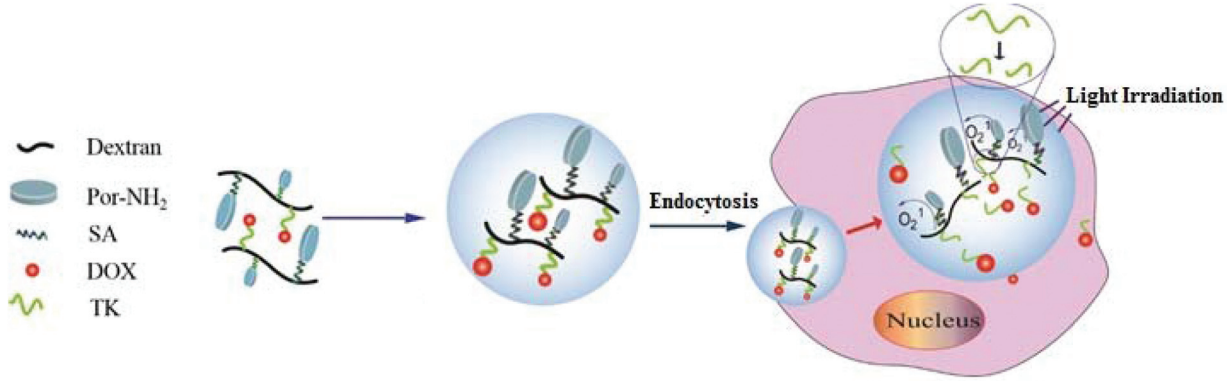


**Scheme 1** Schematic illustration of Por-SA-Dex-TK-DOX conjugates and *in vivo* light-triggered release for combination therapy.

generated ROS would further cleave the ROS-sensitive thioketal linker to achieve ROS-responsive on-demand release of free DOX in the cytosol. PSDTD-3 enhanced the anticancer efficacy of DOX showing the synergistic effect of the chemo-PDT treatment.

According to our previous reports, 5-(4-aminophenyl)-10,15,20-triphenylporphyrin (Por-$NH_2$) was synthesized first. Then, we synthesized succinic anhydride modified Por-$NH_2$ (Por-SA) following the route shown in Scheme S1.† The structure was characterized by $^1$H NMR and FTIR, as shown in Fig. S1 and S2.† Taking advantage of the multiple hydroxyl groups, dextran was chosen as a hydrophilic segment. And then, Por-SA and DOX were conjugated with the dextran backbone with an ester linker and a thioketal linker, respectively. The chemical conjugation of DOX to the polymeric backbone prevented drug leakage without light irradiation in a normal physiological environment. The final porphyrin-based conjugates were synthesized as shown in Schemes S2 and S3.† The structure of Por-SA-Dex-TK-DOX (PSDTD-*m*) was verified using $^1$H NMR and FTIR (Fig. S3–S8†). The amounts of Por and DOX were controlled by the feeding ratio. By adjusting the feeding ratio of DOX, three PSDTD conjugates were prepared, named PSDTD-1, -2, and -3, respectively. The DOX conjugated ratios were 2.5%, 5.6% and 7.2% (as listed in Table 1). The amount of Por was quantified by UV measurement and all three conjugates showed similar Por loading around 13.3%.

When hydrophilic dextran conjugated with hydrophobic drug and photosensitizer, the amphiphilic PSDTD conjugates could self-assemble to form micelles. To study the stability of these micelles, Nile Red was used as a fluorescence probe to measure the critical micelle concentration (CMC). As shown in Table 1, with the increase in the amount of DOX, the CMC value of PDSTD-*m* decreased because of the increased hydrophobicity from DOX. Also, the sizes of the micelles similarly decreased with the increase of DOX as characterized by DLS (Fig. 1A). The polymeric drug conjugate showed a uniform, spherical shape and the size decreased with the increase in DOX, as seen in the TEM image (Fig. 1B–D), which was in agreement with the results from DLS. The stability of the nanoparticles in the physiological environment (pH 7.4) was also analysed by DLS, as shown in Fig. 2A. The conjugate micelles were stable at pH 7.4 in PBS without any significant size change within 48 h. However, when the micelles were irradiated by light, the size of PSDTD-*m* increased over time and the size distribution became broader. We hypothesized that the generated ROS from light irradiation on porphyrin cleaved

**Table 1** The characterization of Por-SA-Dex-TK-DOX conjugates

| Sample | Conjugated ratio of DOX[a] (%) | Grafted ratio of Por[a] (%) | CMC[b] (μg mL$^{-1}$) | $R_h$ (nm) |
|---|---|---|---|---|
| PSDTD-1 | 2.5 | 13.36 | 1.21 | 121.9 ± 4 |
| PSDTD-2 | 5.6 | 13.42 | 0.86 | 90.6 ± 2 |
| PSDTD-3 | 7.2 | 13.39 | 0.74 | 72.3 ± 5 |

[a] Measured and calculated using UV at room temperature. [b] Measured at pH 7.4 in PBS at room temperature.

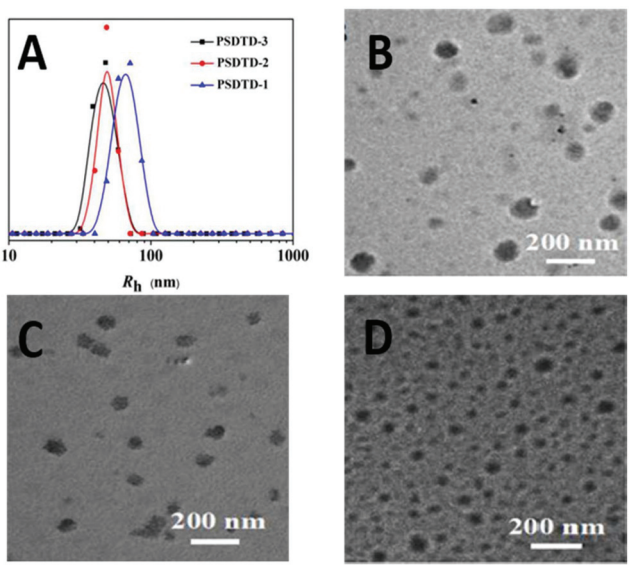


**Fig. 1** The hydrodynamic radii ($R_h$) of PSDTD-*m* (A), and TEM micrographs of PSDTD-1 (B), PSDTD-2 (C) and PSDTD-3 (D).

 

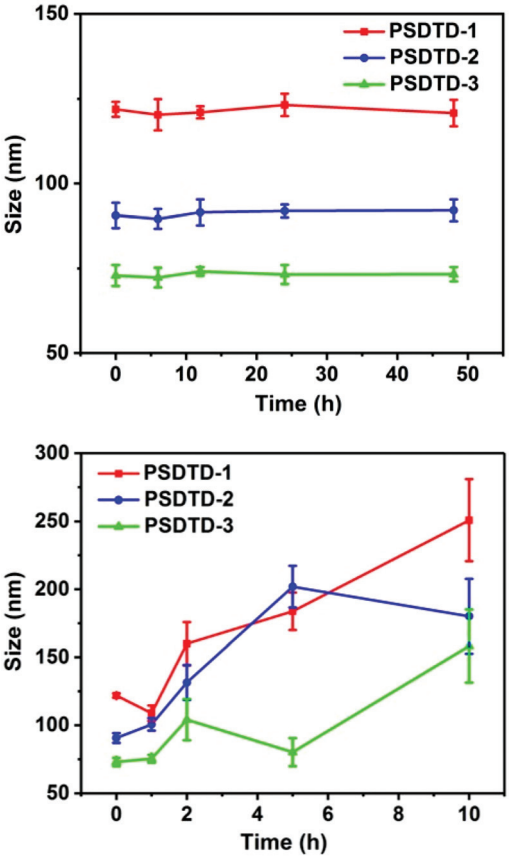


Fig. 2 The stability of PSDTD-*m* within 48 h at pH 7.4 under darkness (A) and under light illumination (B).

the TK linker and led to the release of DOX, which resulted in the micelle size and distribution change (Fig. 2B).

To further verify the light triggered release of DOX from PSDTD-*m*, the *in vitro* release of DOX from the DOX conjugates was investigated. The accumulative release profile of DOX is shown in Fig. 3. It clearly demonstrates that the DOX release behavior closely depends on light irradiation. From the release profile, burst release of DOX was observed after each light irradiation, indicating increased cleavage of the ROS responsive linker by adjacent porphyrin generated ROS after light irradiation. As comparison, 52%, 49% and 41% of DOX were released from PSDTD-3, PSDTD-2 and PSDTD-1, respectively (Fig. S9, S10†), while there was very limited DOX release under darkness. These data indicate that the light irradiation could trigger the drug release under physiological conditions.

Under light irradiation, the amount of ROS generated by the photosensitizer was measured using 9,10-anthracenediyl-bis(methylene)dimalonic acid (ABDA). As shown in Fig. S11–13,† the absorption value of ABDA gradually decreased during the light illumination in the presence of PSDTD, suggesting that the amount of singlet oxygen increased with the increase in the time of illumination. In contrast, the change in the absorption of ABDA was not significant in the absence of conjugates under the same experimental

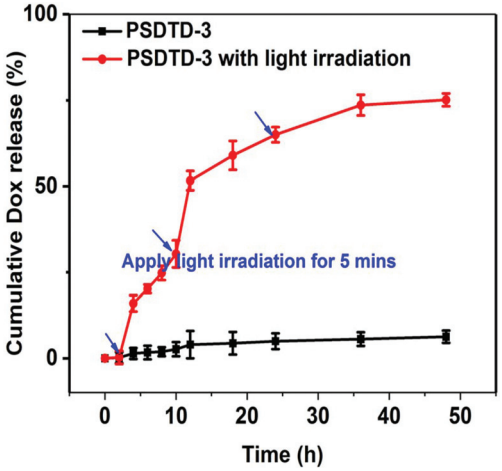


Fig. 3 *In vitro* light triggered DOX release profiles for PSDTD-3 at 37 °C with or without light irradiation.

conditions. The results demonstrated that the decrease in the absorption value of ABDA was due to the presence of PSDTD-*m*, which generated ROS under light irradiation. To monitor the $^1O_2$ generation in living cells under light irradiation, 2,7-dichlorofluorescein diacetate (DCFH-DA) was used as a tracer agent for confocal laser scanning microscopy, because it can be converted to DCFH in living cells, which is oxidized to fluorescent 2,7-dichlorofluorescein (DCF) in the presence of ROS. Compared with the control group (Fig. 4), it was clearly indicated that PSDTD-3 could generate ROS under irradiation.

To evaluate the light controlled release in cancer cells, confocal laser scanning microscopy was exploited to observe the cellular uptake and intracellular drug release behaviour. As indicated in Fig. 5, under light irradiation, red florescence of

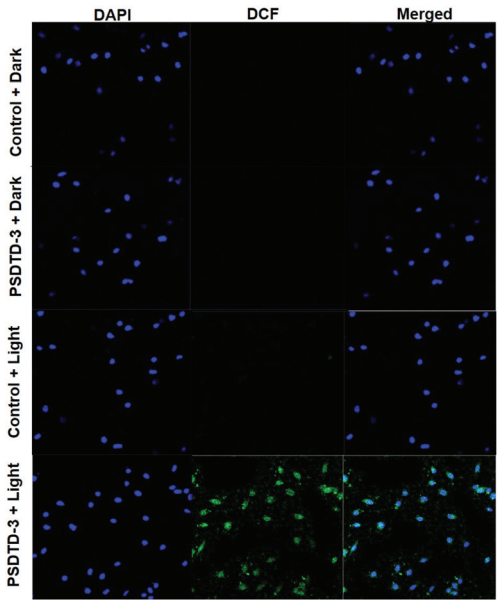


Fig. 4 Intracellular ROS detection of PSDRD-3 with or without light.

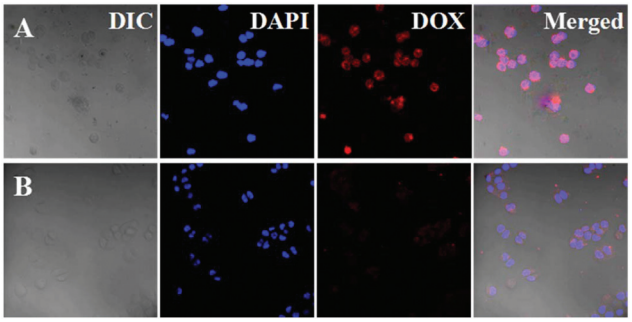


**Fig. 5** Representative CLSM images of HeLa cells incubated in neutral culture medium with PSDTD-3 under light irradiation (A) and without light irradiation (B). For each panel, the figures from left to right show differential interference contrast (DIC) images, cell nuclei stained by DAPI (blue), DOX fluorescence in cells (red), and overlays of the three images.

DOX was observed clearly. Similar results are also found in Fig. S14 and S15† for PSDTD 1 and PSDTD 2. Among all the three PSDTDs, PSDTD-3 treated cells showed the strongest intracellular DOX fluorescence after light irradiation. The intracellular triggered drug release was further monitored by a flow cytometry analysis toward HeLa cells. As shown in Fig. S16–18,† compared with the cells incubated without light irradiation, the cells incubated with PSDTD-1, PSDTD-2 and PSDTD-3 under light irradiation clearly shift to the higher DOX fluorescence intensity indicating improved release of DOX because of the cleavage of the ROS-sensitive linker. The small fluorescence difference observed for PSDTD-*m* without light irradiation was attributed to the different uptake levels of PSDTD micelles. The combined anticancer therapy efficacy of PSDTD-*m* was evaluated by an *in vitro* MTT cytotoxicity assay. As displayed in Fig. 6 and Fig. S19,† the cytotoxicity of PSDTD-3 with light irradiation was higher than that of free DOX with the same dose, indicating the synergistic effect of PDT treatment and intracellular ROS triggered release of DOX. As the control group, PSDTD-3 without light irradiation showed significantly reduced toxicity, demonstrating the decreased off-target side effect of this smart system when an external trigger is not present.

In summary, we constructed light triggered ROS-responsive drug conjugates with dextran as the polymeric backbone for combination of chemo-photodynamic therapy. The photosensitizer was chemically conjugated on the backbone, while the drug was conjugated by a smart ROS-sensitive linker. The light triggered release of DOX from PSDTD-*m* was demonstrated both *in vitro* and in cells. Moreover, the light triggered release of the drug combined with PDT showed enhanced anticancer efficacy upon light irradiation and reduced toxicity when light was absent, proving the strategy of the light triggered smart nanocarrier for enhancing therapy efficacy and lowering side effects.

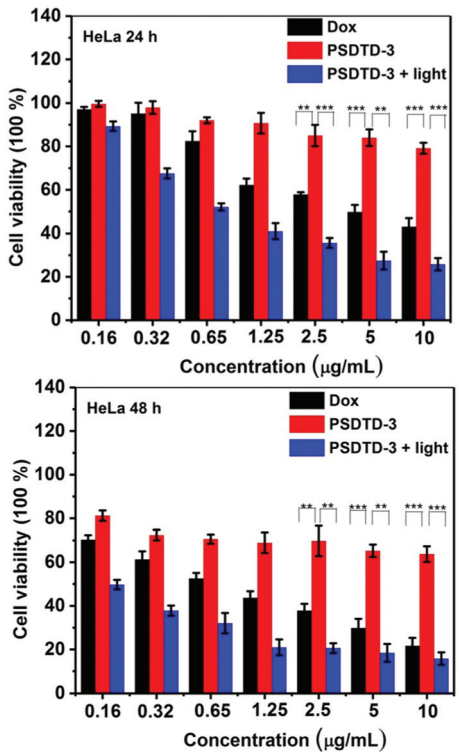


**Fig. 6** Cytotoxicity of free DOX, PSDTD-3 and PSDTD-3 with light irradiation toward HeLa cells after incubation for 24 h and 48 h in neutral culture medium. *$p < 0.05$; **$p < 0.01$; ***$p < 0.001$.

## Conflicts of interest

There are no conflicts to declare.

## Acknowledgements

This research was financially supported by the National Natural Science Foundation of China (Projects 21474012 and 51273037), Jilin Science and Technology Bureau (20130206074GX, International Cooperation Project 20120729), New Century Excellent Talents in University of Jilin Province (2013-6, Jilin Provincial Education Department).

## Notes and references

1 R. J. Browning, P. J. T. Reardon, M. Parhizkar, R. B. Pedley, M. Edirisinghe, J. C. Knowles and E. Stride, *ACS Nano*, 2017, **11**, 8560–8578.
2 Z. Song, Z. Han, S. Lv, C. Chen, L. Chen, L. Yin and J. Cheng, *Chem. Soc. Rev.*, 2017, **46**, 6570–6599.
3 Z. Zhen, W. Tang, C. Guo, H. Chen, X. Lin, G. Liu, B. Fei, X. Chen, B. Xu and J. Xie, *ACS Nano*, 2013, **7**, 6988–6996.
4 H. Ren, J. Liu, F. Su, S. Ge, A. Yuan, W. Dai, J. Wu and Y. Hu, *ACS Appl. Mater. Interfaces*, 2017, **9**, 3463–3473.
5 J. Ding, L. Chen, C. Xiao, L. Chen, X. Zhuang and X. Chen, *Chem. Commun.*, 2014, **50**, 11274–11290.

 

6 S. Lee, S. W. Kang, J. H. Ryu, J. H. Na, D. E. Lee, S. J. Han, C. M. Kang, Y. S. Choe, K. C. Lee, J. F. Leary, K. Choi, K. H. Lee and K. Kim, *Bioconjugate Chem.*, 2014, **25**, 601–610.
7 L. Qiu, T. Chen, I. Ocsoy, E. Yasun, C. Wu, G. Zhu, M. You, D. Han, J. Jiang, R. Yu and W. Tan, *Nano Lett.*, 2015, **15**, 457–463.
8 L. Pan, Q. He, J. Liu, Y. Chen, M. Ma, L. Zhang and J. Shi, *J. Am. Chem. Soc.*, 2012, **134**, 5722–5725.
9 M. H. Teplensky, M. Fantham, P. Li, T. C. Wang, J. P. Mehta, L. J. Young, P. Z. Moghadam, J. T. Hupp, O. K. Farha, C. F. Kaminski and D. Fairen-Jimenez, *J. Am. Chem. Soc.*, 2017, **139**, 7522–7532.
10 T. Lajunen, L. S. Kontturi, L. Viitala, M. Manna, O. Cramariuc, T. Rog, A. Bunker, T. Laaksonen, T. Viitala, L. Murtomaki and A. Urtti, *Mol. Pharm.*, 2016, **13**, 2095–2107.
11 R. D. Airan, R. A. Meyer, N. P. Ellens, K. R. Rhodes, K. Farahani, M. G. Pomper, S. D. Kadam and J. J. Green, *Nano Lett.*, 2017, **17**, 652–659.
12 H. Wang, M. Gauthier, J. R. Kelly, R. J. Miller, M. Xu, W. D. O'Brien Jr. and J. Cheng, *Angew. Chem., Int. Ed.*, 2016, **55**, 5452–5456.
13 S. Guo, Y. Nakagawa, A. Barhoumi, W. Wang, C. Zhan, R. Tong, C. Santamaria and D. S. Kohane, *J. Am. Chem. Soc.*, 2016, **138**, 6127–6130.
14 J. K. Awino, S. Gudipati, A. K. Hartmann, J. J. Santiana, D. F. Cairns-Gibson, N. Gomez and J. L. Rouge, *J. Am. Chem. Soc.*, 2017, **139**, 6278–6281.
15 H. Yang, Q. Wang, S. Huang, A. Xiao, F. Li, L. Gan and X. Yang, *ACS Appl. Mater. Interfaces*, 2016, **8**, 7729–7738.
16 M. R. Jafari, L. Deng, P. I. Kitov, S. Ng, W. L. Matochko, K. F. Tjhung, A. Zeberoff, A. Elias, J. S. Klassen and R. Derda, *ACS Chem. Biol.*, 2014, **9**, 443–450.
17 B. M. Lamb and C. F. Barbas 3rd, *Chem. Commun.*, 2015, **51**, 3196–3199.
18 Q. Meng, J. Meng, W. Ran, J. Su, Y. Yang, P. Zhang and Y. Li, *Chem. Commun.*, 2017, **53**, 12438–12441.
19 M. Bhatti, T. D. McHugh, L. Milanesi and S. Tomas, *Chem. Commun.*, 2014, **50**, 7649–7651.
20 G. Chen, R. Jaskula-Sztul, C. R. Esquibel, I. Lou, Q. Zheng, A. Dammalapati, A. Harrison, K. W. Eliceiri, W. Tang, H. Chen and S. Gong, *Adv. Funct. Mater.*, 2017, **27**, 1604671–1604683.
21 Y. Yuan, Y. Min, Q. Hu, B. Xing and B. Liu, *Nanoscale*, 2014, **6**, 11259–11272.
22 L. Feng, F. He, B. Liu, G. Yang, S. Gai, P. Yang, C. Li, Y. Dai, R. Lv and J. Lin, *Chem. Mater.*, 2016, **28**, 7935–7946.
23 L. Feng, S. Gai, F. He, Y. Dai, C. Zhong, P. Yang and J. Lin, *Biomaterials*, 2017, **147**, 39–52.
24 F. He, G. Yang, P. Yang, Y. Yu, R. Lv, C. Li, Y. Dai, S. Gai and J. Lin, *Adv. Funct. Mater.*, 2015, **25**, 3966–3976.
25 Y. Yuan, J. Liu and B. Liu, *Angew. Chem., Int. Ed.*, 2014, **53**, 7163–7168.
26 X. M. Yao, X. F. Chen, C. L. He, L. Chen and X. S. Chen, *J. Mater. Chem. B*, 2015, **3**, 4707–4714.
27 X. Yao, L. Chen, X. Chen, Z. Zhang, H. Zheng, C. He, J. Zhang and X. Chen, *ACS Appl. Mater. Interfaces*, 2014, **6**, 7816–7822.
28 X. Yao, L. Chen, X. Chen, Z. Xie, J. Ding, C. He, J. Zhang and X. Chen, *Acta Biomater.*, 2015, **25**, 162–171.